LBL-36918
UC-404
Preprint

Lawrence Berkeley Laboratory
UNIVERSITY OF CALIFORNIA

Materials Sciences Division

Submitted to Journal of the American Ceramic Society

In Situ Toughened Silicon Carbide With Al-B-C Additions

J.J. Cao, W.J. MoberlyChan, L.C. De Jonghe,
C.J. Gilbert, and R.O. Ritchie

March 1995

U. C. Lawrence Berkeley Laboratory
Library, Berkeley

FOR REFERENCE

Not to be taken from this room

REFERENCE COPY
Does Not
Circulate
Bldg. 50 Library.
LBL-36918
Copy 1

Prepared for the U.S. Department of Energy under Contract Number DE-AC03-76SF00098

DISCLAIMER

This document was prepared as an account of work sponsored by the United States Government. While this document is believed to contain correct information, neither the United States Government nor any agency thereof, nor the Regents of the University of California, nor any of their employees, makes any warranty, express or implied, or assumes any legal responsibility for the accuracy, completeness, or usefulness of any information, apparatus, product, or process disclosed, or represents that its use would not infringe privately owned rights. Reference herein to any specific commercial product, process, or service by its trade name, trademark, manufacturer, or otherwise, does not necessarily constitute or imply its endorsement, recommendation, or favoring by the United States Government or any agency thereof, or the Regents of the University of California. The views and opinions of authors expressed herein do not necessarily state or reflect those of the United States Government or any agency thereof or the Regents of the University of California.

LBL-36918

In Situ Toughened Silicon Carbide With Al-B-C Additions

J. J. Cao, W. J. MoberlyChan, L. C. De Jonghe, C. J. Gilbert, and R. O. Ritchie

Department of Materials Science and Mineral Engineering
University of California

and

Material Science Division
Lawrence Berkeley Laboratory
University of California
Berkeley, California 94720

March 1995

This work was supported by the Director, Office of Energy Research, Office of Basic Energy Sciences, Materials Sciences Division, of the U. S. Department of Energy under Contract No. DE-AC03-76SF00098.

In Situ Toughened Silicon Carbide With Al-B-C Additions

J. J. Cao[+], W. J. MoberlyChan, L. C. De Jonghe[+], C. J. Gilbert[+], and R. O. Ritchie

Center for Advanced Materials, Materials Sciences Division, Lawrence Berkeley Laboratory, and Department of Materials Science and Mineral Engineering, University of California, Berkeley, CA 94720-1760

Abstract *"In situ* toughened" silicon carbides, containing Al, B, and C additives, were prepared by hot pressing. Densification, phase transformations, and microstructural development are described. The microstructures, secondary phases, and grain boundaries were characterized using a range of analytical techniques including TEM, SEM, AES, and XRD. The modulus of rupture was determined from four-point bend tests, while the fracture toughness was derived either from bend tests of beam-shaped samples with a controlled surface flaw, or from standard disk-shaped compact-tension specimens pre-cracked in cyclic fatigue. The R-curve behavior of an *in situ* toughened SiC was also examined. A steady-state toughness over 9 $MPa{\cdot}m^{1/2}$ was recorded for the silicon carbide prepared with minimal additives under optimum processing conditions. This increase in fracture toughness, over a factor of three compared to that of a commercial SiC, was achieved while maintaining a bend strength of 650 MPa. The mechanical properties were found to be related to a microstructure in which plate-like grain development of α- SiC

Supported by the Director, Office of Energy Research, Office of Basic Energy Sciences, Materials Sciences Division of the U.S. Department of Energy, under Contract No. DE-AC03-76SF00098.

[+] member, American Ceramic Society.

had been promoted, and where crack bridging by intact grains was a principal source of toughening. [Key words: silicon carbide, toughening, crack bridging, R-curve, beta-to-alpha transformation]

1. Introduction

The advantages of silicon carbide in high temperature structural applications include high strength, creep resistance, and chemical stability. A disadvantage, however, has been its low fracture toughness, typically of 2 to 4 $MPa \cdot m^{1/2}$. A number of attempts have recently been made to improve the fracture toughness of this ceramic, with toughness values reported as high as 6 to 8 $MPa \cdot m^{1/2}$. These efforts include toughening by heterophase dispersion,[1,2] by incorporation of coated α-SiC platelets in a β-SiC matrix,[3-5] and by addition of Al_2O_3[6-8] or Al_2O_3-Y_2O_3.[9-12] The aims of the latter efforts were to achieve a plate-like microstructure in which grain bridging and crack deflection were promoted by the presence of substantive amounts of the additives.[6-8,10-12] This provided an *in situ* toughened material with a microstructure akin to that of tough silicon nitride. Suzuki,[6] using alumina as an additive, and later Mulla and Krstic,[7] produced a microstructure consisting of elongated α-SiC grains. The materials showed a modulus of rupture (MOR) of about 600 MPa, and a fracture toughness of 5 to 6 $MPa \cdot m^{1/2}$ determined by the single edge notched-beam method (with no pre-cracking). Silicon carbides with alumina-yttria additives were prepared by Lee and Kim,[10] and more recently by Padture *et al.*[11,12] These materials, containing 10 to 26 wt% YAG, were reported to

exhibit fracture toughnesses of ~8 $MPa \cdot m^{1/2}$, as determined by the Vickers indentation method.[10,11]

The objective of the present work was to augment the toughening of SiC using aluminum metal, boron, and carbon in relatively low concentrations as sintering aids. This combination of additives, under processing conditions described here, favorably affected the microstructure and phase transformation characteristics, and yielded a silicon carbide with a steady-state fracture toughness in excess of 9 $MPa \cdot m^{1/2}$ while at the same time retaining a high modulus of rupture. The mechanical properties, evaluated at room temperature, and the related microstructural characteristics were compared to those of a baseline commercial SiC ceramic (Hexoloy SA).

2. Experimental Procedure

Submicron β-SiC[i], with a mean particle size of 0.15 μm, was mixed with Al-B-C additives in toluene. The Al-metal[ii], which had an average particle size of 3 μm, constituted from 1 to 6 wt% of the powder. For all mixtures prepared, the boron[iii] content was kept at 0.6 wt%. The carbon was introduced as 4 wt% Apiezon wax[iv], which was converted upon pyrolysis to yield ~2 wt% C.

---

[i] BSC-21, Ferro Co., Cleveland, OH.
[ii] H-3, Valimet, Stockton, CA.
[iii] Callery Chemical Co., Callery, PA.
[iv] Biddle Instruments, Plymouth Meeting, PA.

The slurries of SiC powder with additives were ultrasonically agitated for five minutes, and passed through a 325 mesh sieve. Following stir-drying, the mixture was re-ground in a mortar and pestle and screened through a 200 mesh sieve. After cold die-compression at 35 MPa, the green compacts were hot pressed in graphite dies lined with graphite foil, at temperatures between 1700°C and 1950°C, for 15 minutes to 4 hours, at 50 MPa, under flowing argon. Three disks, 38 mm in diameter and 4 mm thick, were fabricated during each processing run, using graphite spacers between specimens.

Densities of the hot pressed specimens were determined by Archimedes' method. Optical, X-ray, and electron beam methods were used for the microstructural and chemical characterization. These methods included optical microscopy (OM), X-ray diffraction (XRD), scanning electron microscopy (SEM), conventional and high resolution transmission electron microscopy (TEM and HR-TEM). Compositional information was obtained from energy dispersive spectroscopy (EDS), wavelength dispersive X-ray analysis (WDS), parallel electron energy loss spectroscopy (PEELS), and Auger electron spectroscopy (AES).

The basic mechanical properties of the silicon carbides were evaluted on beams of 2.7 by 3 by 30 mm sectioned from the hot pressed billets. The beams were tested in a 4-point bending jig with an outer span of 25.4 mm, an inner span of 9.5 mm, at a crosshead speed of 0.05 mm/min. The tensile surfaces of the specimens had been polished to a ~1 μm diamond finish, and the tensile edges were beveled to reduce edge flaws. For fracture

toughness measurements, a controlled surface flaw was introduced on the tensile surface with a Knoop indenter, using a load between 98 N and 137 N. The fracture toughness was calculated from the relation:[13,14]

$$K_c = \frac{2.06}{\sqrt{\pi}} \sigma_f \sqrt{a} \qquad (1)$$

where "σ_f" is the fracture stress and "a" is the initial flaw radius of the indentation measured on the fracture surface with an SEM. For each processing condition, four beams were used to measure the average fracture toughness K_c, and at least five beams were tested to determine modulus of rupture (MOR).

The fracture toughness and resistance-curve (R-curve) behavior of an optimised silicon carbide was also evaluated using an ASTM E399 standard disk-shaped compact-tension DC(T) specimen of width W = 28.6 mm and thickness B = 3.26 mm. Prior to data collection, the specimen was pre-cracked under cyclic loading[i]. Crack lengths were continuously monitored using a combination of several methods, including electrical-potential measurements across a thin (~100 nm) NiCr film evaporated onto the specimen surface, compliance measurements using a 350 Ω strain gauge attached to the back face of the specimen, and direct size measurment with a high-resolution optical traveling microscope. Details of these experimental techniques have been reported elsewhere.[15] Before measuring the resistance-curve, the specimen was cycled for ~24 hours at a sufficiently low ΔK such that no crack growth was detected over this interval. This

[i] The fatigue pre-crack was made under cyclic loading at 25 Hz with a sinusoidal wave form on a computer controlled servo-hydraulic testing machine several millimeters beyond the wedge-shaped starter-notch at an applied stress intensity range of $\Delta K = 7\ MPa \cdot m^{1/2}$, with load ratio $R = K_{min}/K_{max} = 0.1$.

precaution minimized the effect on the measured initiation toughness K_o of any pre-existing damage and crack-tip shielding[ii]. Subsequently, the resistance curve was measured by bringing the specimen to failure under load control at a rate of ~0.05 $MPa \cdot m^{1/2}/sec$.

3. Results and Discussion

3.1 Processing and Microstructural Development

The densities of the silicon carbides, hot pressed at 1700°C and at 1900°C respectively, have been plotted versus the added content of metallic aluminum in Figure 1. The combination of Al, B, and C as sintering additives has evidently been effective for densification. When silicon carbide was hot pressed at 1700°C, 3 wt% Al was sufficient to reach nearly full density; whereas at 1900°C, only 1 wt% Al was needed. The effectiveness of Al as a sintering aid for SiC has been evidenced e.g. in the previous work of De Jonghe *et al.*[3-5] in which β-SiC, containing up to ~32 vol% of oxide-coated α-SiC platelets, was hot pressed to near full density at temperatures below 1700°C.

X-ray diffraction spectra from the polished surfaces of the hot pressed SiC with 3wt%Al-0.6wt%B-2wt%C additions and processed at different temperatures have been

[ii] In grain-bridging ceramics, frictional wear in the interfaces between interlocking grains that span the crack during cyclic fatigue loading can lead to an almost complete degradation of crack bridging in the crack wake. See references 16 and 17.

shown in Figure 2 , together with the spectrum of the β-SiC starting powder. After processing at 1700°C, the SiC remained mainly as the β-phase (3C); the peak broadness, however, was significantly reduced from that of the original powders, indicating that the β-phase grains had grown. The β-to-α phase transformation was essentially complete after hot pressing at 1950°C: the relative XRD intensities of this specimen had a near perfect match with those of a 4H-SiC standard,[18] indicating at the same time that the 4H grains were randomly distributed. No other SiC polytypes (*e.g.*, 6H or 15R) were evident at any temperature. Favored formation of the 4H polytype in Al-containing SiC had been reported by Hamminger *et al.*[19] when studying the structures of several pressureless sintered SiC compositions. Shinozaki *et al.*[20-22] also found that the 3C to 4H phase transformation was enhanced by the presence of Al together with B and C. However, Shinozaki *et al.* reported that the 3C-SiC transformed to 4H-SiC through an intermediate structure of 15R, which was not observed in the present study (neither by XRD nor by TEM). The differences in crystal structures of the transformation products were believed to originate in the differences in the starting β-SiC powders. Pure crystalline β-phase powders were used here, while Shinozaki *et al.*[20-22] used powders containing 29% of a "disordered" phase. A β-SiC seeded with 0.5 wt% of sub-micron 6H-SiC hot pressed at 1900°C for 15 minutes formed 30 % of 6H, 40 % of 4H, with 3C as the balance (see Table 1). The minimal addition of 6H seeds caused substantial 3C to 6H transformation, or more appropriately, the growth of the 6H grains. A direct transformation of the 3C to 4H has also been reported with Y_2O_3-Al_2O_3 additives.[10]

When only B and C were used as additives, the β-to-α phase transformation began at temperatures greater than 1950°C.[23-25] The addition of a small amount of metallic aluminum or aluminum compounds lowered this phase transformation temperature. Onset of the β-to-α phase transformation has been reported at approximately 1800°C with 1.5wt%Al-1.2wt%B-4wt%C additions.[21,22] In the present study, 3 wt% of metallic Al with 0.6 wt% B and 2 wt% C was found to promote strongly the β-to-α phase transformation by further lowering the onset temperature. A trace of 4H-SiC was detected at a hot pressing temperature as low as 1700°C by both XRD and TEM. Hot pressing at 1780°C for 1 hour caused 20% 3C to 4H transformation (Table 1), as determined using the method of Ruska *et al.*[18] After hot pressing at 1900°C, 75% 4H formed, and at 1950°C the transformation was complete.

Figures 3a through 3c show TEM images of microstructures of SiC hot pressed with 3wt%Al-0.6wt%B-2wt%C at 1700°C, 1780°C, and 1900°C, respectively. As the sintering temperature increased, the SiC grains grew into plate-like shapes. Cross-sectional grain length, grain width, and aspect ratios were measured for at least 50 grains in TEM images or in SEM micrographs of etched surfaces, and the results are listed in Table 2. For plate-like grains, the aspect ratios determined from two dimensional measurements tends to underestimate the true aspect ratios in three dimensions. It was also noted that numerous small grains (< 0.2 μm) were observed in the microstructures for silicon carbides processed at 1700°C and 1780°C. Because these small grains were believed not

to contribute to toughening and strengthening, they were not included in the measurements reported in Table 2.

The growth of plate-like grains was found to be associated with the 3C to 4H phase transformation. The silicon carbide hot pressed at 1700°C showed a duplex grain structure with approximately two-thirds of the material being β-phase grains of about one micron in length by half micron in width, while the other one-third of the material consisted of β grains, an order of magnitude smaller in size. A few large grains in this SiC had larger aspect ratios, and electron diffraction determined these grains to be of a dual structure (*i.e.*, partially 3C and partially 4H). When processed at 1780°C, the majority of the grains had plate-like shapes, and showed the dual grain structures. At 1900°C, the grains had grown longer, and the portion of the 4H-phase increased. After hot pressing at 1950°C, the grains were larger both in length and in width, and exhibited only the 4H-phase. The origin and growth mechanism of the dual grain structures is not clear at this time and has been left as the subject of a future study.

Figure 4a is an SEM micrograph of a polished surface of a hot pressed SiC containing 6wt%Al-0.6wt%B-2wt%C. The high Al content was intended to exaggerate the formation of secondary phases. The silicon carbide matrix appears gray, while various secondary phases are relatively brighter or darker. This contrast is likely to originate from the differences in conductivity of the various phases, as all contrast vanished when a thin conductive gold coating was applied to the surface. Energy dispersive and wavelength

dispersive X-ray spectroscopy (EDS and WDS) showed that the secondary phase regions contained Al and were free of Si. WDS further revealed that the bright secondary phases contained oxygen, while the dark secondary phases did not. Figures 4b-d show wavelength dispersive X-ray maps of Al, Si, and O respectively, obtained on the polished surface imaged in Figure 4a. AES further determined that the dark secondary phases were mainly aluminum-boron-carbides, with a few being aluminum carbides, while the bright regions were aluminum oxides and aluminum oxycarbides. Electron diffraction and lattice imaging by TEM have confirmed the existence of these secondary phases.[4] Graphite inclusions, often reported in SiC with B and C additions,[21,26] were not observed. The silicon carbides discussed in section 3.3 of this paper contained 3 wt% Al, and had much smaller amounts of secondary phases, with the major inclusions determined to be $Al_8B_4C_7$ by TEM and AES.

The formation of secondary phases was attributed to the sintering additives present in concentrations well above their solubilities in SiC. The solubility limit reported for aluminum in SiC is 0.26wt% and 0.50wt% at 1800°C and 2000°C respectively, and for boron it is 0.1 wt% at 2500°C.[27] Thus, secondary phases should be expected to form, especially as the Al melts well below the processing temperatures. In the presence of the added aluminum, carbon, and boron, together with oxygen from the powder surfaces, several phases are thermodynamically possible. Examples are $Al_8B_4C_7$, which has a melting point near 1800°C;[28] and Al_4O_4C, which has an eutectic reaction with Al_2O_3 at 1840°C.[29]

Ternary and quaternary phase diagrams among elements of Si, Al, B, C, and O have been shown elsewhere.[4]

The possible presence of liquid phases at grain boundaries was expected to play a major role in densification and grain growth. A high resolution lattice image of two neighboring grains in specimen B3 is shown in Figure 5, revealing an amorphous grain boundary phase of less than one nanometer thick. An Auger electron spectrum, acquired from an intergranular fracture surface, showed the presence of Si, C, Al, O (Figure 6a). After sputtering away less than one nanometer of material from this surface, the Al and O signals disappeared (Figure 6b). The Si and C signals were from the bulk SiC; the O signal could be from absorped oxygen, since the specimen was fractured in air. It can be concluded at this point that the grain boundary phase contained Al; however, the exact chemistry of the grain boundary phase has not yet been determined with certainty.

Sintering of the present Al, B, and C-doped SiC was believed to be a liquid phase process, similar to that for the Al_2O_3-added SiC described by Suzuki.[6] A likely scenario that could be envisioned was as follows. During heating, metal aluminum melted, and B, C, and O were presumed to transport into the aluminum melt and form secondary phases. The liquid phase(s) flowed, filling pores between the nearby SiC particles and engulfing many grains, as observed by TEM.[4] Meanwhile, aluminum vapor coated the SiC particle surfaces, and reacted with the native oxide on the powder surface as well as the added carbon and boron to form a liquid grain boundary phase. In the presence of an applied

pressure, particle rearrangement occurred. A liquid phase sintering mechanism, *i.e.*, a solution-reprecipitation process, caused gradual densification coupled with grain growth. At this stage, corresponding to sintering at ≤ 1700°C with 3 wt% or more Al addition, a fine-grained dense 3C-SiC was obtained. At higher sintering temperatures, SiC transformed from 3C to 4H, accompanied by the formation and growth of plate-like grains with increasing aspect ratios. At temperatures above 1900°C, however, grain growth of 4H-SiC continued while the 3C phase gradually diminished, while at the same time the grain aspect ratios decreased.

An optimal microstructure, in terms of high-aspect-ratio plate-like grains with grain boundary phases less than one nanometer thick, was produced by hot pressing at 1900°C. Figure 7 shows optical and SEM micrographs of the SiC etched by boiling in Murakami's reagent (10 g of NaOH and 10 g of $K_3Fe(CN)_6$ in 100 mL H_2O) for 45 minutes. Plate-like grains are shown here; apparent porosity in these microstructures resulted from etching damage and from the preferential removal of secondary phases. A TEM micrograph and an Auger electron spectrum of this sample was shown in Figure 3c and Figure 6, respectively.

3.2 Mechanical Properties

Figures 8a and 8b show the fracture toughness (measured from bend tests with a controlled surface flaw) and four-point bend strength of the silicon carbides hot pressed

between 1700°C and 1950°C, for 1 hour, with 3wt%Al-0.6wt%B-2wt%C additions. Since fracture toughness values are sensitive to the particular testing methodology,[30] similar measurements were made on a commercial SiC (Hexoloy SA) for comparison. When the sintering temperature increased from 1700°C to 1900°C, the fracture toughness increased from 3.2 to 6.8 $MPa \cdot m^{1/2}$. The latter value is over 3 times higher compared to that of Hexoloy SiC. As measured from the fatigue pre-cracked DC(T) specimen, the SiC hot pressed at 1900°C for 1 hour exhibited significant resistance-curve behavior (Figure 9), rising from an initiation value of K_o = 5.5 $MPa \cdot m^{1/2}$ to a plateau value of K_c =9.1 $Mpa \cdot m^{1/2}$. The maximum crack growth resistance was reached after ~600 μm of crack extension. Such behavior has been attributed to extensive crack bridging by the *in situ* grown plate-like grains, as is discussed below. The fracture toughness of Hexoloy SiC was determined by similar methods to be 2.5 $Mpa \cdot m^{1/2}$, and no resistance-curve behavior was detected using a pre-cracked DC(T) specimen.

Because crack length was monitored continuously throughout the resistance-curve measurement, the K_c from the measurement using the DC(T) geometry may be considered to be a more representative value. The significant variation between K_c measured from the DC(T) geometry and K_c using the controlled surface flaw method for specimen B3 (9.1 compared to 6.8 $MPa \cdot m^{1/2}$) can be attributed to several factors associated with the latter technique. In the present bend tests with controlled surface flaws, the residual stresses near the pre-crack from Knoop indentation[13] were not removed; as a result, the measured values of fracture toughness were consistently lower

than those obtained by more conventional methods.[13,31] This was evident when considering the apparently low value of 2.2 $MPa \cdot m^{1/2}$ measured here for Hexoloy SiC, where 2.7 $MPa \cdot m^{1/2}$ has been reported when residual stresses were removed by surface polishing.[32] In some instance, a fracture toughness as high as 4 $MPa \cdot m^{1/2}$ has been cited for the Hexoloy.[11] In addition, a conservative assumption was made here in Equation (1) that the pre-crack was semi-circular. If ellipticity of the pre-crack (in fact, this was observed) had been included, a toughness value higher than that calculated from equation (1) would have been obtained.[13,14] More importantly, the pre-crack from Knoop indentation was typically 200 to 250 μm, which is in the "small crack" range, meaning that toughness measurements using the controlled surface flaw method yield an essentially arbitrary point on the R-curve, invariably below the steady-state value.

As the hot pressing temperature was raised from 1700°C to 1900°C, the average bend strength increased slightly, and the scatter of the measured data decreased significantly (Figures 8a and 8b). The standard deviation of strength was reduced from 90 MPa (~15%) to 20 MPa (~3%). Above 1900°C, however, the bend strength decreased, presumably as a result of larger pre-existing flaws induced by excessive grain growth.

To examine the effect of sintering time on fracture toughness and bend strength, silicon carbides were hot pressed and held at 1900°C for times ranging from 15 minutes to 4 hours (Figure 10). As the hot-pressing time increased, the fracture toughness increased while the strength slightly decreased. These changes were believed to originate in the

differences in grain size. The increasing scatter in measured toughness was mostly the result of the increasing difficulty in measuring the pre-crack length in the coarser microstructures.

Fracture toughnesses and bend strengths have been plotted versus grain length in Figure 11a. This plot indicates that some degree of grain growth was beneficial for both toughness and strength. Upon increasing the grain length from ~1 μm to ~9 μm, the fracture toughness increased by more than a factor of 2; for an increase in the grain length from ~1 μm to ~5 μm, some improvement in strength was also observed. From elementary fracture mechanics, it is known that strength relates to toughness and flaw size. The strength increase with grain growth was presumably the result of the much improved toughness. In Figure 11b the fracture toughness and bend strength are plotted versus the aspect ratios of the plate-like grains. The fracture toughness increased from ~3 to ~7 $MPa \cdot m^{1/2}$ when the aspect ratio increased from ~3 to ~9. The strength, however, was not sensitive to the aspect ratio.

Figures 12a through 12d shows fractographs of silicon carbides hot pressed at various temperatures. At relatively low sintering temperatures (1700°C and 1780°C), the fracture mode was predominantly intergranular. When sintered at 1900°C, some transgranular fracture occurred; however, intergranular fracture still dominated, with the majority of the plate-like grains exhibiting pullout. At 1950°C, the material showed a larger fraction of transgranular fracture, particularly for the larger grains. In comparison,

the fracture surface of Hexoloy SiC exhibited complete transgranular fracture, as is evident in Figure 12e.

Toughening in these silicon carbides was primary attributed to grain bridging and subsequent grain pullout. Partially debonded plate-like grains, which resided just behind the crack tip, bridged the crack, thereby reducing the effective stress intensity.[33] With very fine grains (for example, after hot pressing at 1700°C), toughening from grain bridging and pullout was minimal. After hot pressing at higher temperatures (*e.g.*, at 1900°C), growth of the plate-like grains with increased aspect ratio highly enhanced the effect of crack bridging, resulting in a significant improvement in fracture toughness and, to a lesser extent, in strength.

Another contribution to the overall toughening was expected from crack deflection. This mechanism of toughening is known to be governed by the aspect ratio of the elongated grains[34] which is plotted in Figure 11b. The crack path from a Vickers indent is shown in Figure 13a, where crack deflection has been marked by arrow 1 and grain pullout by arrow 2. On the other hand, the indentation crack path is quite straight in Hexoloy SiC as shown in Figure 13b.

The optimal mechanical properties, in terms of both high fracture toughness and strength, were achieved by hot pressing at 1900°C, coinciding with conditions where the

optimal microstructure was obtained. The physical and mechanical properties of the SiC hot pressed at 1900°C for one hour have been summarized in Table 3.

4. Conclusions

Hot pressed SiC ceramics with Al-B-C additives have been produced and evaluated. Through a liquid phase mechanism, dense SiC was obtained by hot pressing at a temperature as low as 1700°C (with ≥ 3wt%Al). In addition, the 3C (β) to 4H (α) phase transformation began at this temperature with 3wt%Al-0.6wt%B-2wt%C additions, and completed at 1950°C. In association with the 3C to 4H phase transformation, the SiC grains grew into plate-like shapes. A thin (< 1 nm) Al-containing amorphous grain boundary phase was detected by HR-TEM and analyzed by AES. Grain bridging, pullout, and crack deflection accounted for an improvement in fracture toughness over three times that of a commercial SiC. The *in situ* toughened SiC exhibited a significant rising R-curve behavior with a steady-state fracture toughness over 9 $MPa \cdot m^{1/2}$, while retaining a high modulus of rupture (~650 MPa).

Acknowledgment

We are grateful to Dr. B. J. Dalgleish for his assistance in the mechanical testing.

REFERENCES

[1]G. Wei and P. Becher, "Improvements in Mechanical Properties in SiC by the Addition of TiC Particles," J. Am. Ceram. Soc., **67** [8] 571-74 (1984).

[2]Y. Ohya, M. J. Hoffmann, and G. Petzon, "Sintering of in-situ Synthesized SiC-TiB_2 Composites with Improved Fracture Toughness," J. Am. Ceram. Soc., **75** [9] 2479-83 (1992)

[3]T. Mitchell, Jr., L. C. De Jonghe, W. J. MoberlyChan, and R. O. Ritchie, "Silicon Carbide Platelet / Silicon Carbide Composites," J. Am. Ceram. Soc., **78** [1] 97-103 (1995).

[4]W. J. MoberlyChan, J. J. Cao, M. Y. Niu, and L. C. De Jonghe, "Toughened β-SiC Composites with Alumina-Coated α-SiC Platelets," in High Performance Composites----Commonalty of Phenomena, edited by K. K. Chawla, P. K. Liaw, and S. G. Fishman, TMS Publication, pp. 219-29, 1994.

[5]J. J. Cao, W. J. MoberlyChan, L. C. De Joughe, B. Dalgleish, and M. Y. Niu, "Processing and Characterization of SiC Platelet / SiC Composites," Advances in Ceramic-Matrix Composites II, Ceramic Transactions, Vol. 46, pp. 277-88, 1995.

[6]K. Suzuki, "Pressureless-Sintered Silicon Carbide with Addition of Aluminum Oxide," in Silicon Carbide Ceramics--2. Edited by S. Somiya and Y. Inomata. Elsvier Applied Science, NY, NY, pp.162-82, 1991.

[7]M. A. Mulla and V. D. Krstic, "Mechanical Properties of β-SiC Pressureless Sintered with Al_2O_3 Additions," Acta Metall. Mater., **42** [1] 303-08 (1994).

[8]S. S. Shinozaki, J. Hangas, K.R. Carduner, M. J. Rokosz, K. Suzuki, and N. Shinohara, "Correlation Between Microstructure and Mechanical Properties in Silicon Carbide with Alumina Addition," J. Mater. Res., **8** [7] 1635-43 (1993).

[9]M. A. Mulla and V. D. Krstic, "Low-Temperature Pressureless Sintering of β-Silicon Carbide with Aluminum Oxide and Yttrium Oxide Additions," Am. Ceram. Soc. Bull., **70** [3] 439-43 (1991).

[10]S. K. Lee and C. H. Kim, "Effects of α-SiC versus β-SiC Starting Powders on Microstructure and Fracture Toughness of SiC Sintered with Al_2O_3-Y_2O_3 Additives," J. Am. Ceram. Soc., **77** [6] 1655-58 (1994).

[11]N. P. Padture, "*In Situ*-Toughened Silicon Carbide," J. Am. Ceram. Soc., **77** [2] 519-23 (1994).

[12]N. P. Padture and B. R. Lawn, "Toughness Properties of a Silicon Carbide with an in Situ Induced Heterogeneous Grain Structure," J. Am. Ceram. Soc., **77** [10] 2518-22 (1994).

[13]J. J. Petrovic and M. G. Mendiratta, "Fracture from Controlled Surface Flaw," Fracture Mechanics Applied to Brittle Materials, ASTM STP 678. S. W. Freiman, Ed., American Society for Testing and Materials, pp. 83-102, 1979.

[14]P. C. Paris, and G. C. Sih, "Stress Analysis of Cracks," Fracture Toughness Testing and Its Applications, ASTM STP. 381, pp. 30-81, 1965.

[15]R. H. Dauskardt and R. O. Ritchie, "Cyclic Fatigue-Crack Growth Behavior in Ceramics," Closed Loop, **17** [2] 7-17 (1989).

[16]R. H. Dauskardt, "A Frictional-Wear Mechanism for Fatigue-Crack growth in Grain Bridging Ceramics," Acta Metall. Mater., **41** [9] 2765-81 (1993).

[17]C. J. Gilbert, R. H. Dauskardt, R. W. Steinbrech, R. N. Petrany, and R. O.Ritchie, "Cyclic Fatigue in Monolithic Alumina: Mechanism of Crack Advance Promoted by Frictional Wear of Grain Bridges," J. Mater. Sci., **30** [2] 643-54 (1995).

[18]J. Ruska, L. J. Gauckler, J. L. Lorenz, and H. U. Rexer, "The Quantitative Calculation of SiC Polytypes from Measurements of X-Ray Diffraction Peak Intensities," J. Mater. Sci., **14** [8] 2013-17 (1979).

[19]R. Hamminger, G. Grathwohl, and F. Thummler, "Microanalytical Investigation of Sintered SiC," J. Mater. Sci., **18** [2] 353-64 (1983).

[20]S. Shinozaki, J. Hangas, K. Maeda, and A. Soeta, "Enhanced Formation of 4H Polytype in Silicon Carbide Materials," Silicon Carbide'87, J. D. Cawley and C. E. Semler Ed., Ceramic Transactions, Vol. 2, pp. 113-21, 1987.

[21]S. Shinozaki, R. M. Williams, B. N. Juterbock, W. T. Donlon, J. Hangas, and C. R. Peters, "Microstructural Developments in Pressureless-Sintered β-SiC Materials with Al, B, and C Additions," Am. Ceram. Soc. Bull., **64** [10] 1389-93 (1985).

[22]R. M. Williams, B. N. Juterbock, S. Shinozaki, C. R. Peters, and T. J. Whalen, "Effects of Sintering Temperatures on the Physical and Crystallographic Properties of β-SiC," Am. Ceram. Soc. Bull., **64** [10] 1385-89 (1985).

[23]M. Srinivasan, "The Silicon Carbide Family of Structural Ceramics," in Structural Ceramics, Edited by J. B. Wachtman, Jr., Treatise on Materials Science and Technology, Vol. 29, pp. 99-159, Academic Press, Inc., 1989.

[24]A. H. Heuer, G. A. Fryburg, L. U. Ogbuji, T. E. Mitchell, and S. Shinozaki, "β→α Transformation in Polycrystalline SiC: I, Microstructural Aspects," J. Am. Ceram. Soc., **61** [9-10] 406-12 (1978).

[25]L. U. Ogbuji, T. E. Mitchell, and A. H. Heuer, "β→α Transformation in Polycrystalline SiC: III, Thickening of α Plates," J. Am. Ceram. Soc., **64** [2] 91-99 (1981).

[26]R. A. Bishop and H. K. Bowen, "Suspension Processing of Beta-SiC Powders," Silicon Carbide'87, J. D. Cawley and C. E. Semler Ed., Ceramic Transactions, Vol. 2, pp. 157-73, 1987.

[27]Y. Tajima and W. D. Kingery, "Solubility of Aluminum and Boron in Silicon Carbide," J. Am. Ceram. Soc., **65** [2] C27-29 (1982).

[28]Y. Inomata, H. Tanaka, Z. Inoue, and H. Kawabata, "Phase Relation in SiC-Al_4C_3-B_4C System at 1800°C," J. Ceram. Soc. Japan, **88** (6), 353-55 (1980).

[29]L. M. Foster, G. Long, and M. S. Hunter, "Reactions Between Aluminum Oxide and Carbon," J. Am. Ceram. Soc., **39** [1] 1-11 (1956).

[30]I. Merkel and U. Messerschmidt, "Fracture Toughness of Sintered SiC Ceramics: A Comparison Between Different Methods," Mat. Sci. Eng., **A151** [2] 131-35 (1992).

[31]J. J. Petrovic, L. A. Jacobson, P. K. Talty, and A. K. Vasudevan, "Controlled Surface Flaws in Hot-Pressed Si_3N_4," J. Am. Ceram. Soc., **58** [3-4] 113-66 (1975).

[32]Private communication with B. J. Dalgleish, Lawrence Berkeley Laboratory, Berkeley, CA.

[33]P. F. Becher, "Microstructural Design of Toughened Ceramics," J. Am. Ceram. Soc., **74** [2] 255-69 (1991).

[34]K. T. Faber and A. G. Evans, "Crack Deflection Processes--I. Theory," Acta Metall. **31** [4] 565-76 (1983).

CAPTIONS

Fig.1 Densities of silicon carbides hot pressed at 1700°C and 1900°C with various amounts of Al, together with 0.6wt%B and 2wt%C additives.

Fig.2 X-ray diffraction spectra of the starting β-SiC powder and of silicon carbides hot pressed at various temperatures with 3wt%Al-0.6wt%B-2wt%C additives.

Fig.3 TEM micrographs of silicon carbides hot pressed at various temperatures with 3wt%Al-0.6wt%B-2wt%C additives: (a) 1700°C, (b) 1780°C, and (c) 1900°C.

Fig.4 SEM micrograph (a) and wavelength dispersive X-ray maps of Al (b), Si (c), and O (d) of a polished specimen with 6wt%Al-0.6wt%B-2wt%C additives.

Fig.5 High resolution TEM micrograph shows lattice image of two neighboring grains in specimen B3, indicating an amorphous grain boundary phase of less than one nanometer thick.

Fig.6 Auger electron spectrum acquired of an intergranular fracture surface (a), and of the same area after ion sputtering less than one nanometer of material from the surface (b).

Fig.7 Optical (a) and SEM micrographs (b) of an etched surface of specimen B3, showing elongated SiC grains.

Fig.8 Fracture toughness (measured from bend tests with a controlled surface flaw) (a) and four-point bend strength (b) of silicon carbides hot pressed between 1700°C and 1950°C with 3wt%Al-0.6wt%B-2wt%C additions. Measured data for Hexoloy SiC are included for comparison.

Fig.9 A crack growth resistance-curve of K_R as a function of crack extension Δa for specimen B3, in comparison to the behavior of Hexoloy SiC. Note the very high plateau (steady-state) fracture toughness of 9.1 $MPa \cdot m^{1/2}$.

Fig.10 Fracture toughness K_c (determined from bend tests with a controlled surface flaw) and four-point bend strength MOR as a function of hot-pressing time at 1900°C.

Fig.11 Fracture toughness K_c (determined in bend tests with a controlled surface flaw) and four-point bend strength MOR as a function of grain length (a) and as a function of grain aspect ratio (b) in hot pressed silicon carbides.

Fig.12 SEM fractographs of silicon carbides hot pressed at various temperatures: (a) 1700°C/1hr, (b) 1780°C/1hr, (c) 1900°C/1hr, (d) 1950°C/1hr, and (e) Hexoloy SiC.

Fig.13 SEM images of crack paths from Vickers indentation in (a) an *in situ* toughened SiC, and (b) Hexoloy SiC. Note the bridged (as shown by arrow 1) and deflected (arrow 2) path in (a), versus the straight and transgranular path in (b). The horizontal arrow shows direction of crack growth.

Table 1. Processing Conditions and SiC Polytypes

Material	Starting powder	Sintering aides	Hot-press conditions	SiC polytypes
B1	#100(3C)	3Al-0.6B-2C	1700°C/1hr	*100(3C), <1(4H)
B2	100(3C)	3Al-0.6B-2C	1780°C/1hr	80(3C), 20(4H)
B3	100(3C)	3Al-0.6B-2C	1900°C/1hr	25(3C), 75(4H)
B4	100(3C)	3Al-0.6B-2C	1950°C/1hr	100(4H)
A1	99.5(3C), 0.5(6H)	3Al-0.6B-2C	1900°C/15 min.	30(3C), 40(4H), 30(6H)

Weight percentages of the starting powder of each SiC polytypes as indicated in parentheses.

* Volume percentage calculated based on XRD using the method by Ruska *et al.*[18]

Table 2. Processing Conditions, Microstructural Results, and Mechanical Properties of Hot-Pressed Silicon Carbides with 3wt%Al-0.6wt%B-2wt%C Additions

Material	Hot-press Temp.	Density (g/cm^3)	SiC Length(μm)	Grain Width(μm)	Size Aspect ratio	MOR (MPa)	K_C[i] ($MPa \cdot m^{1/2}$)
B1	1700°C	3.19	1.0 (0.5)*	0.4 (0.2)	2.8 (0.9)	600 (90)	3.2 (0.1)
B2	1780°C	3.19	2.7 (0.9)	0.7 (0.3)	4.0 (1.4)	650 (70)	4.4 (0.2)
B3	1900°C	3.18	5.5 (2.4)	0.7 (0.2)	7.6 (2.3)	660 (20)	6.8 (0.4)
B4	1950°C	3.18	13.3 (3.6)	2.6 (0.9)	5.4 (1.6)	540 (50)	6.0 (0.2)
Hexoloy[#]	N/A[+]	3.14	~5	~5	~1	400 (40)	2.2 (0.1)

Note: * Data in the parentheses indicate standard deviation.

[#] Commercial SiC (Hexoloy SA) from Carborundum, Niagara Falls, NY.

[+] Sintering temperature has not been reported.

[i] K_C was measured using the controlled surface flaw method in four point bending, without removing residual stresses. This tends to underestimate the fracture toughness, as is discussed in section 3.3. The steady-state fracture toughness of sample B3 was determined to be 9.1 $MPa \cdot m^{1/2}$ using fatigue pre-cracked disk-shaped compact-tension specimens.

Table 3. Processing Conditions and Properties of an *in situ* Toughened Silicon Carbide

Sintering additives	3wt%Al-0.6wt%B-2wt%C
Hot pressing conditions	1900°C / 1 hr
Density	3.18 g/cm^3
Crystal structure	75% (4H) + 25% (3C)
Grain size (cross sectional)	
Length	5.5+/- 2.4 μm
Width	0.7 +/- 0.2 μm
Aspect ratio	7.6 +/- 2.3
Hardness (Vickers, 500 g load)	24.0 +/- 1.7 GPa
Four-point bend strength	660 +/- 20 MPa
Fracture toughness	
Four-point bending with controlled-surface flaw	6.8 +/- 0.3 MPa·m$^{1/2}$
DC(T) with fatigue pre-crack	9.1 MPa·m$^{1/2}$

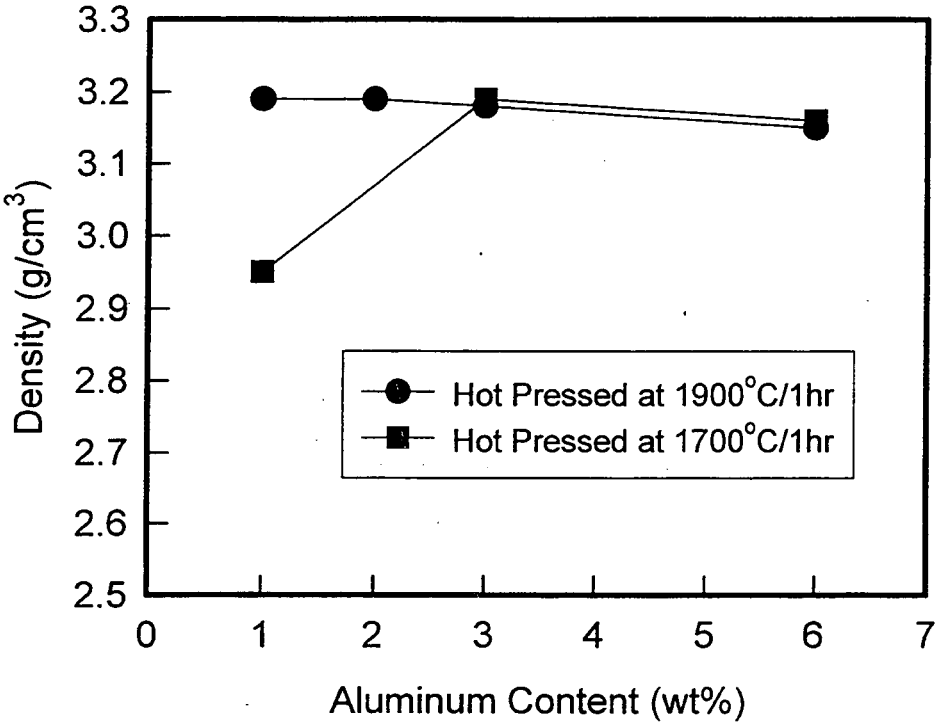

Figure 1 Densities of silicon carbides hot pressed at 1700°C and 1900°C with various amounts of Al together with 0.6wt%B-2wt%C additives.

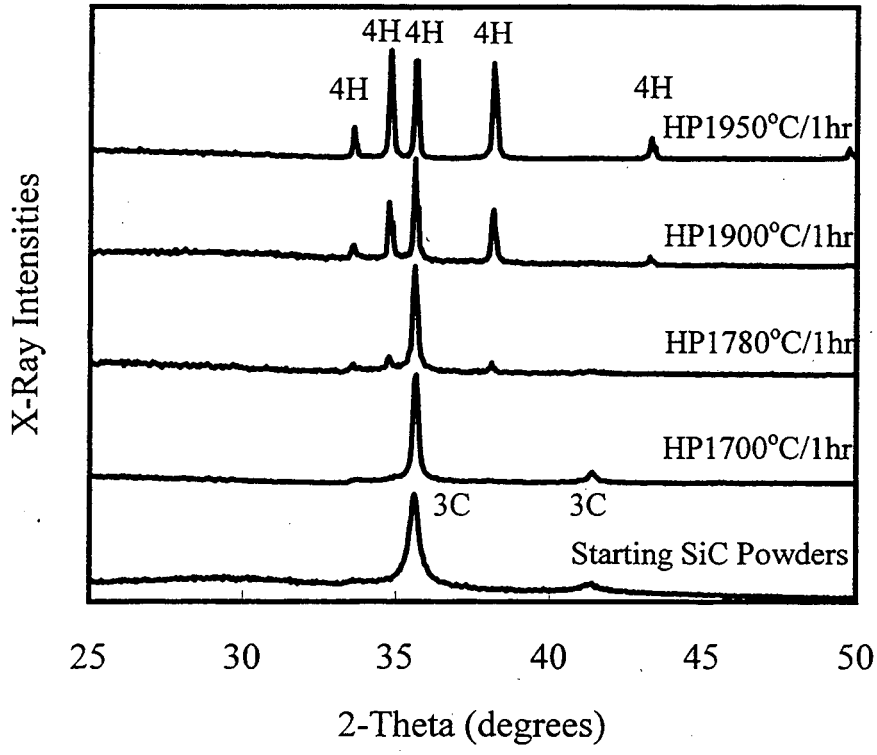

Figure 2 X-ray diffraction patterns of the starting beta-SiC Powder and of silicon carbides hot pressed at various temperatures, for one hour, with 3wt%Al-0.6wt%B-2wt%C additions.

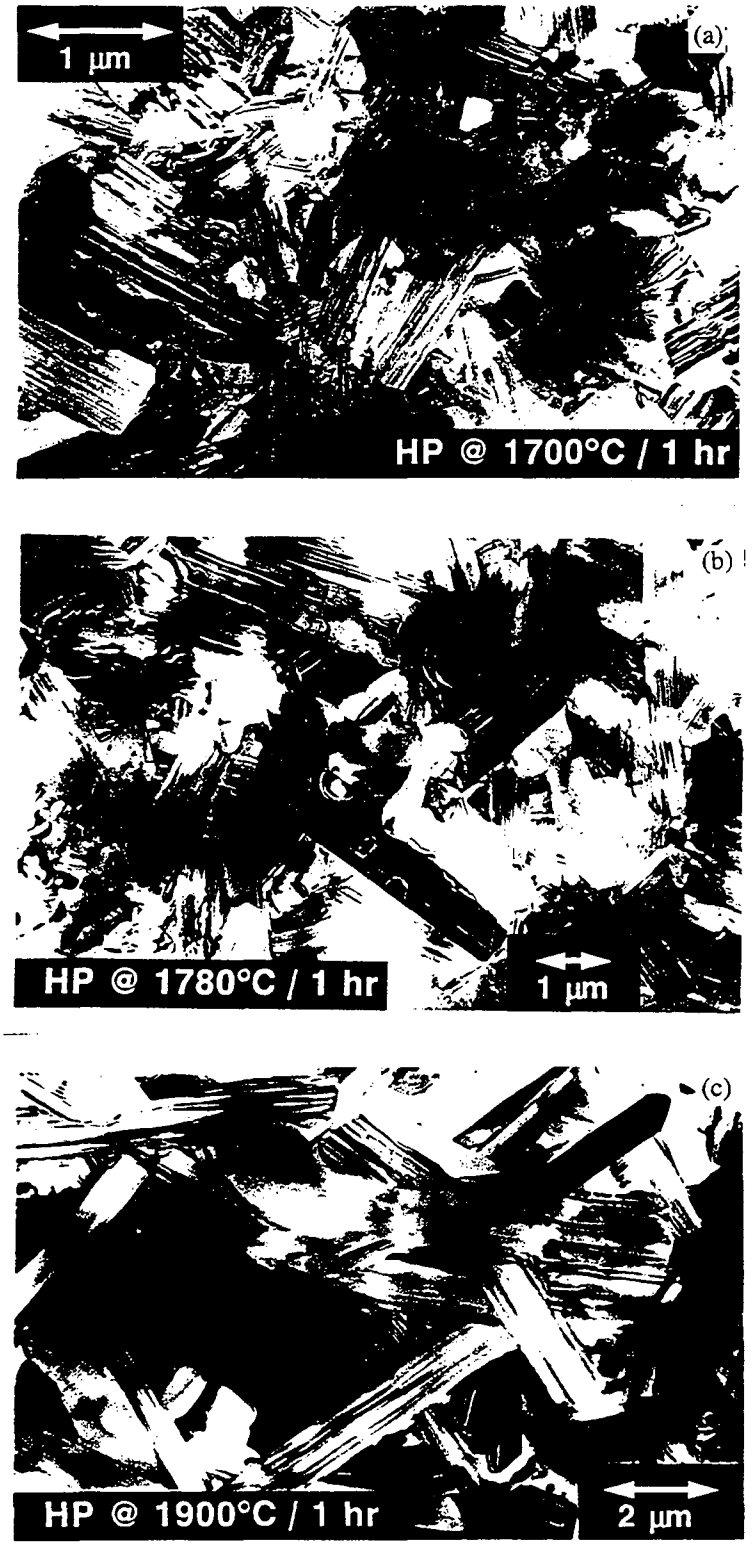

Fig.3 TEM micrographs of silicon carbides hot pressed at various temperatures with 3wt%Al-0.6wt%B-2wt%C additives: (a) 1700°C, (b) 1780°C, and (c) 1900°C.

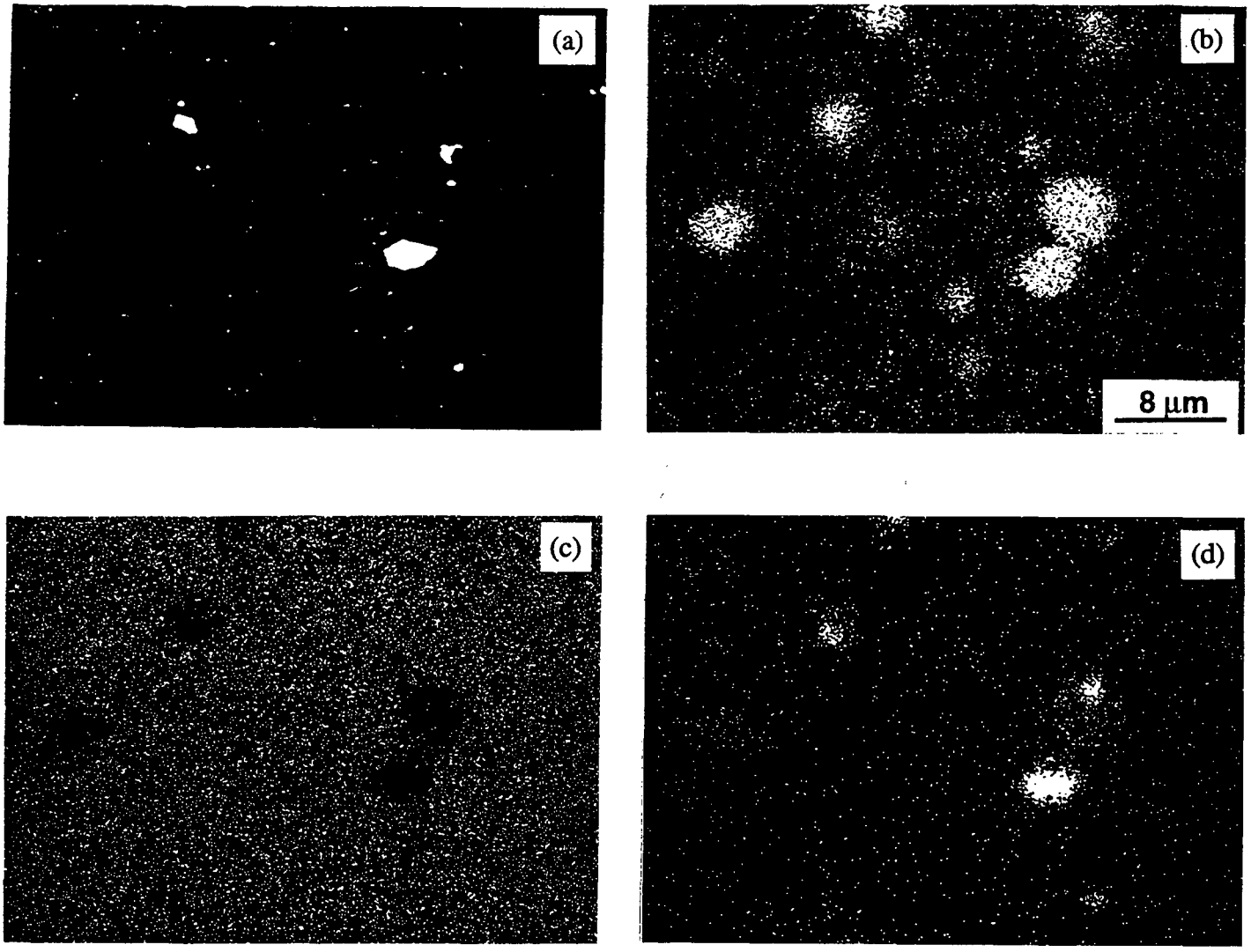

Figure 4 SEM micrograph (a) and wavelength dispersive X-ray maps of Al (b), Si (c), and O (d) of a polished specimen with 6wt%Al-0.6wt%B-2wt%C additives.

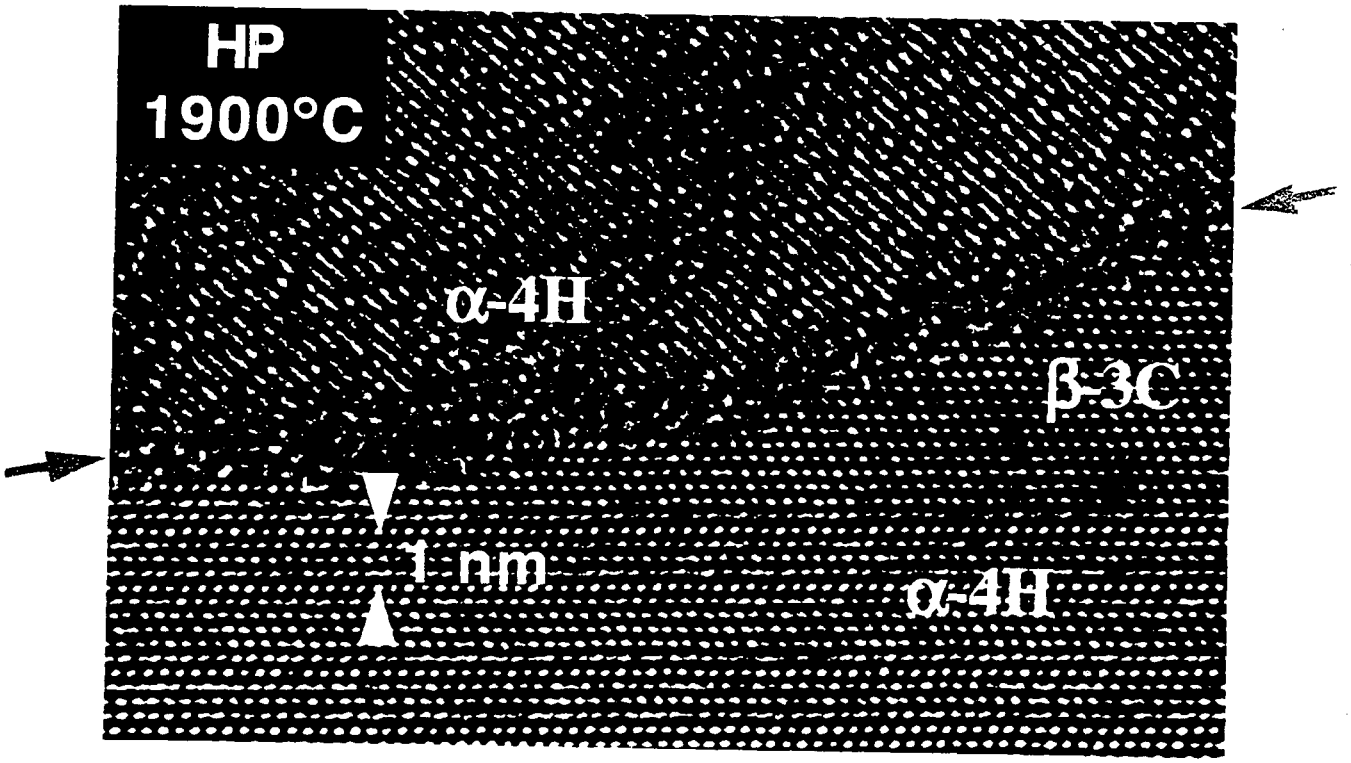

Fig.5 High resolution TEM micrograph shows lattice image of two neighboring grains in specimen B3, indicating an amorphous grain boundary phase of less than one nanometer thick.

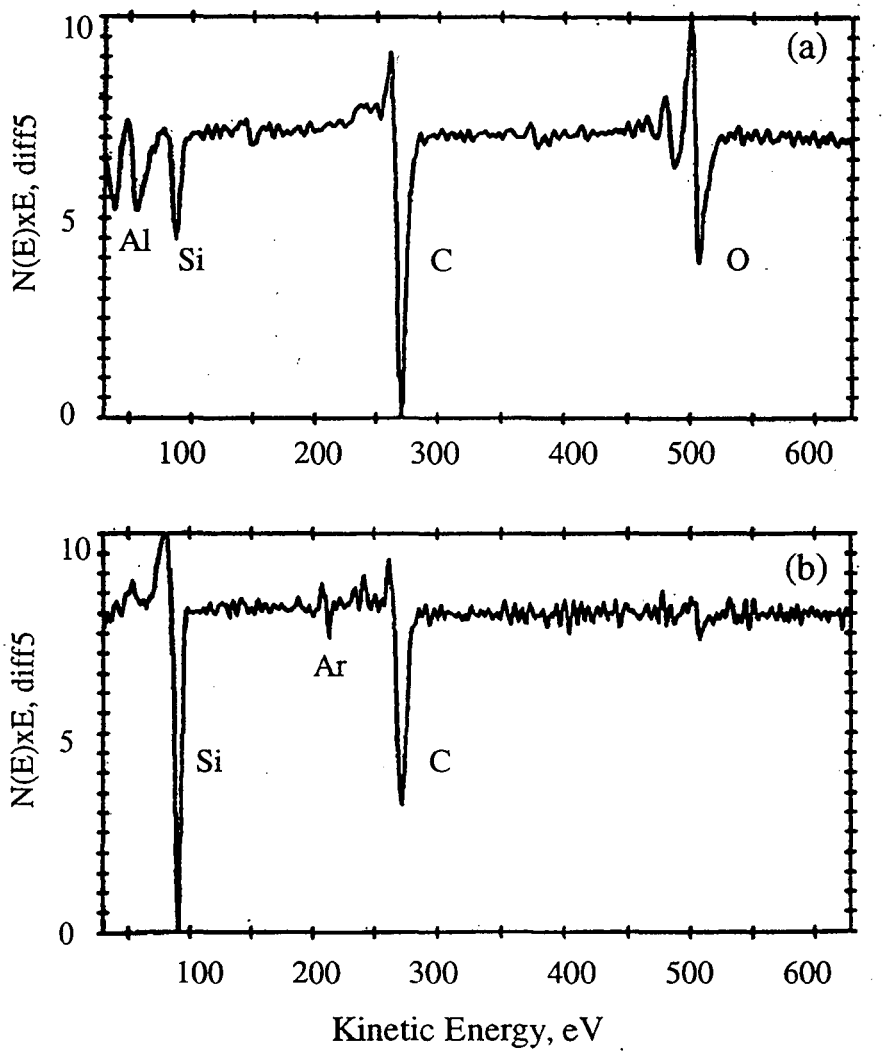

Figure 6 Auger electron spectrums aquired of an intergranular fracture surface (a), and of the same area after ion sputtering less than one nanometer of material from the surface (b).

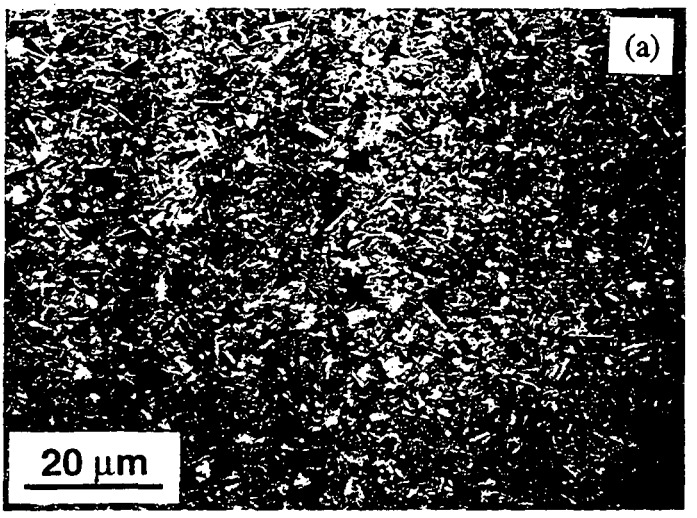

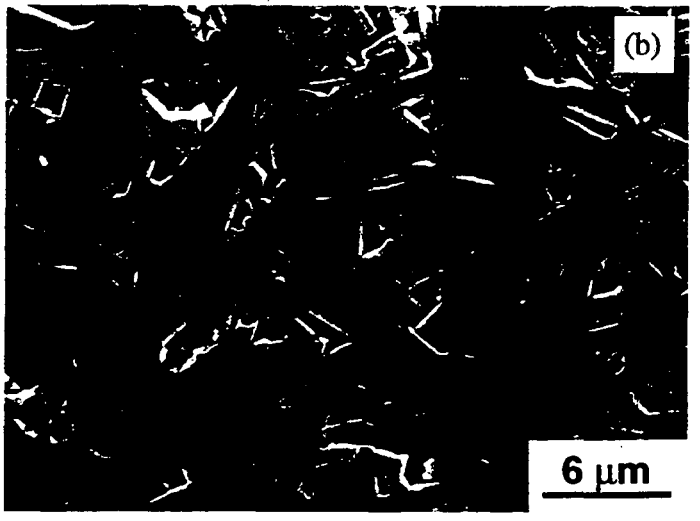

Figure 7 Optical (a) and SEM micrographs (b) of an etched surface of specimen B3, showing elongated SiC grains.

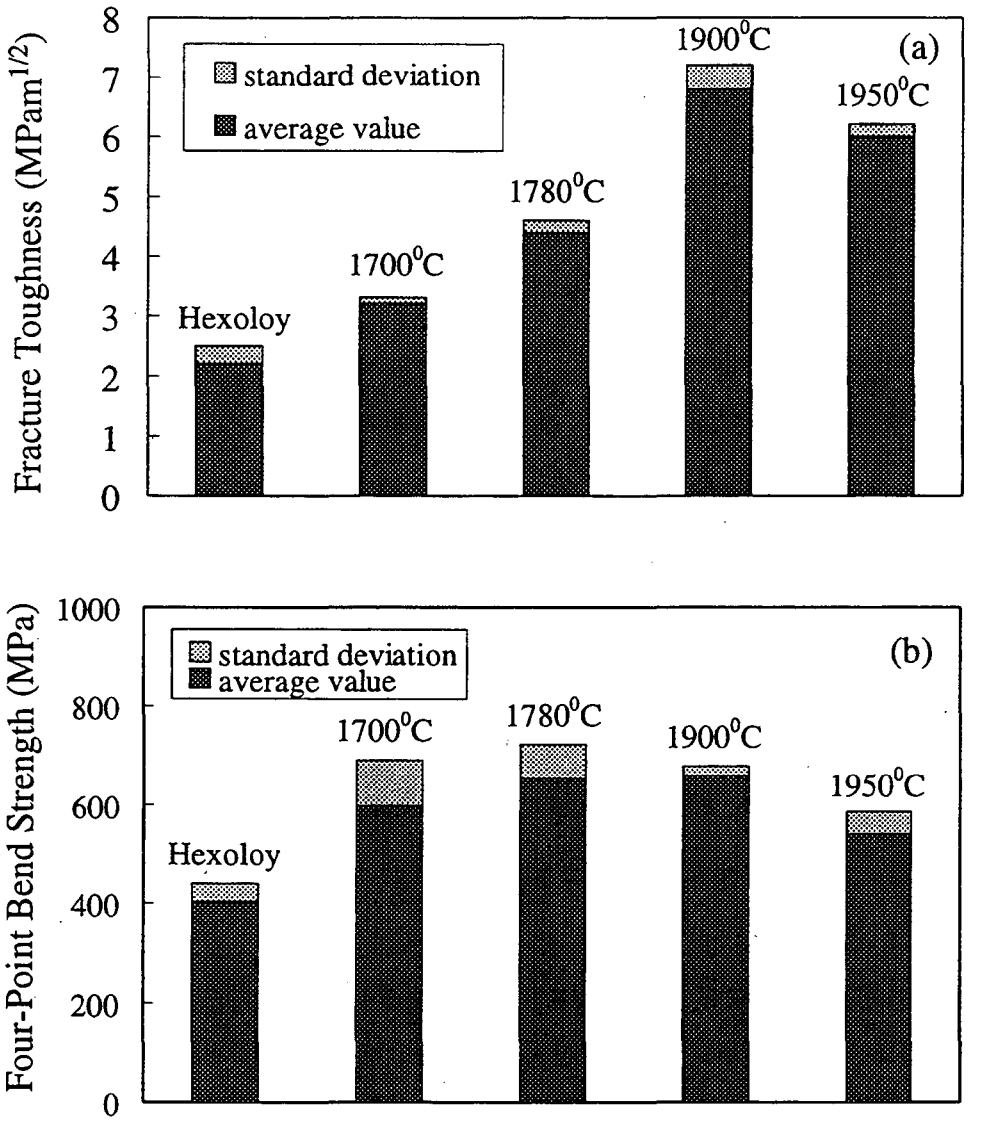

Figure 8 Fracture toughness (determined from bend tests with a controlled surface flaw) (a) and four-point bend strength (b) of silicon carbides hot pressed at various temperatures. Measured data for Hexoloy SiC are included for comparison.

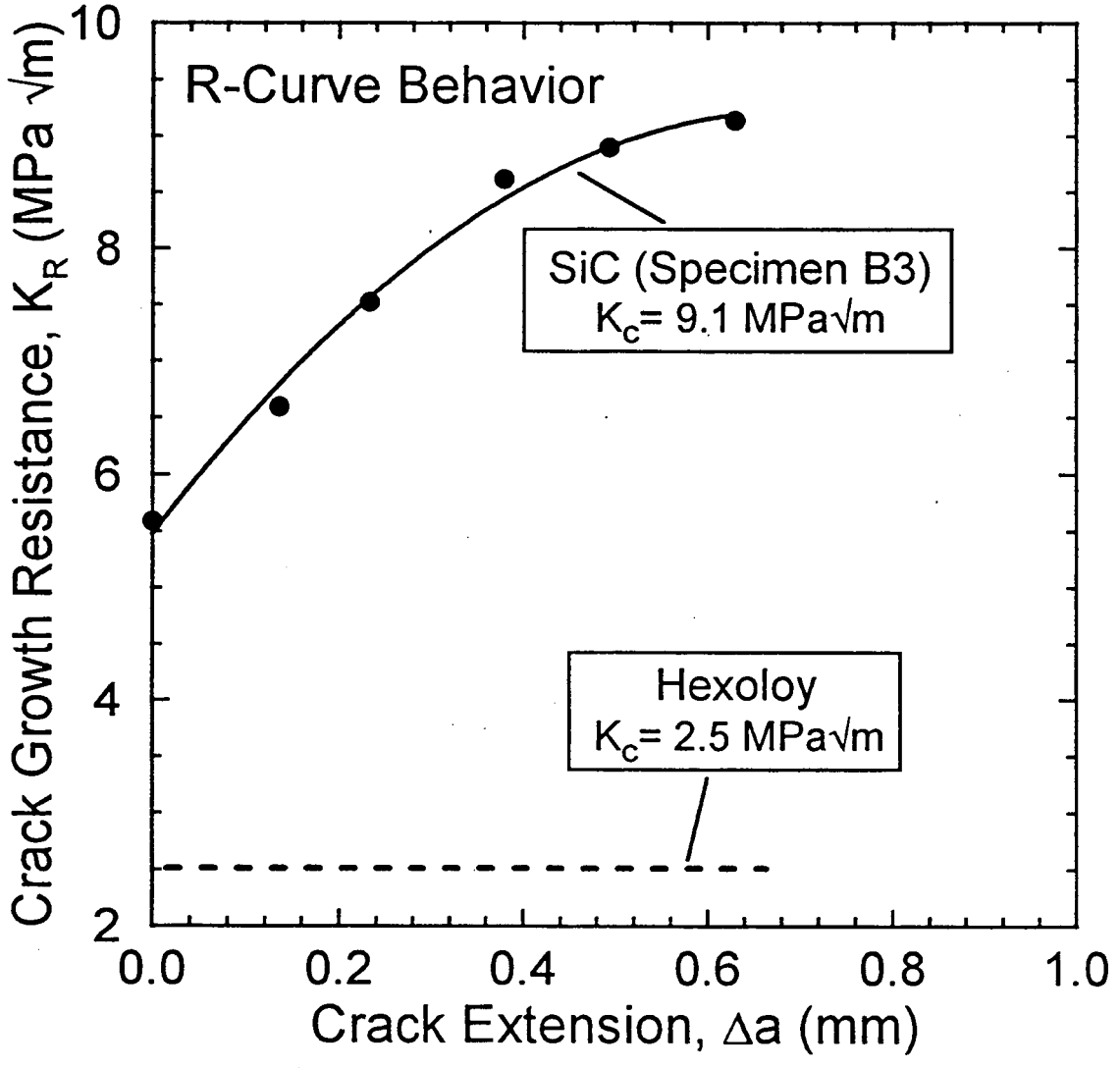

Fig.9 A crack growth resistance-curve of K_R as a function of crack extension Δa for specimen B3, in comparison to the behavior of Hexoloy SiC. Note the very high plateau (steady-state) fracture toughness of 9.1 $MPam^{1/2}$.

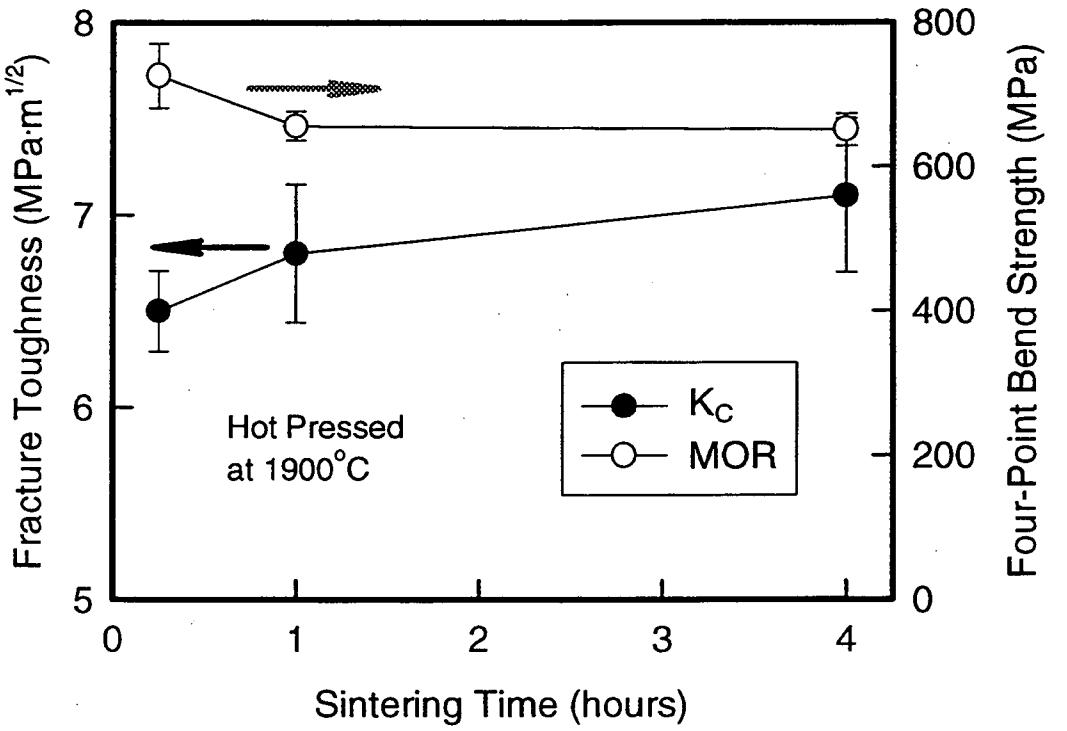

Figure 10 Fracture toughness K_C (determined from bend tests with a controlled surface flaw) and bend strength MOR as a function of hot pressing time at 1900°C.

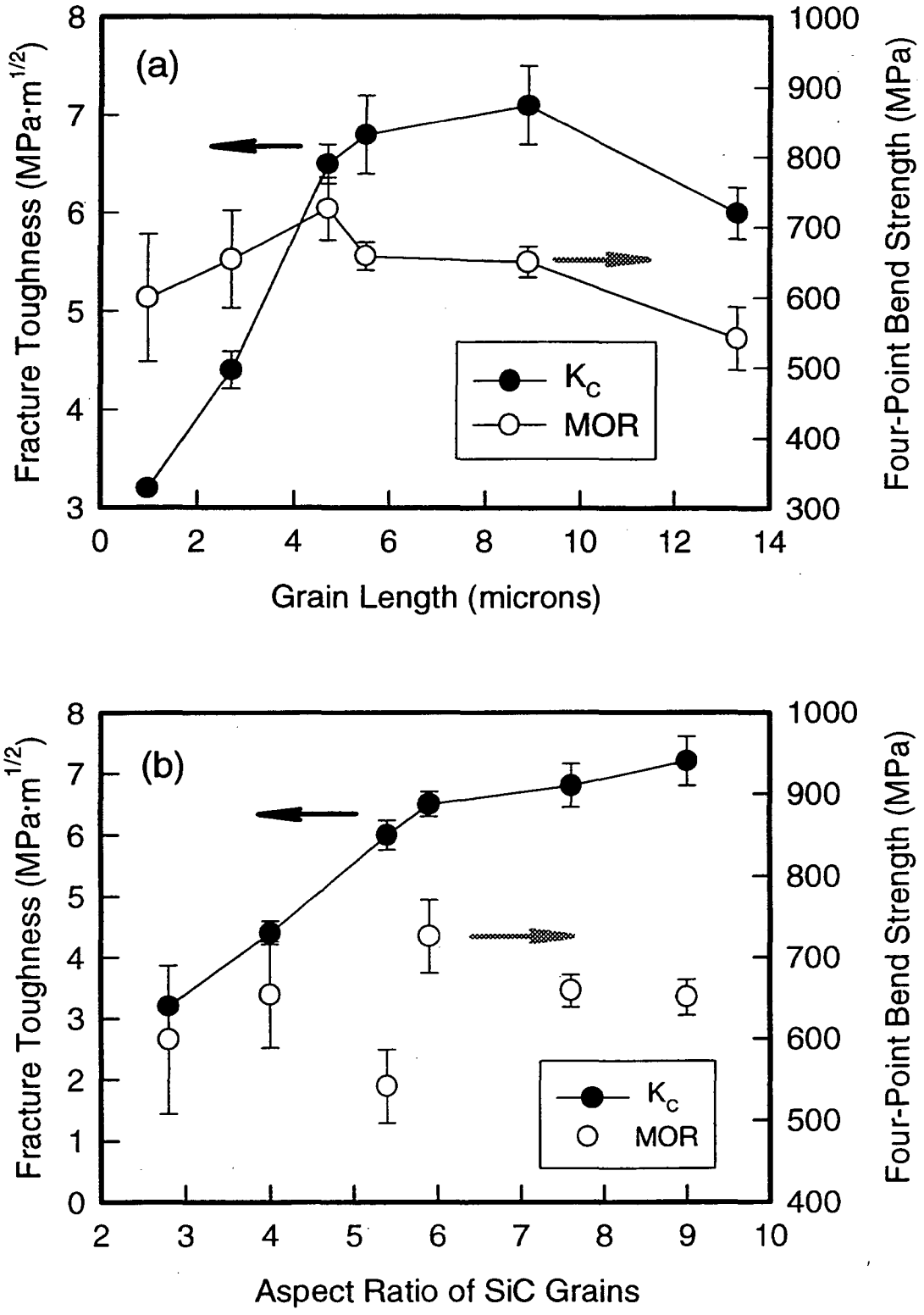

Figure 11 Fracture toughness K_C (determined from bend tests with a controlled surface flaw) and bend strength MOR as a function of grain length (a) and as a functigrain aspect ratios (b) of hot pressed silicon carbides.

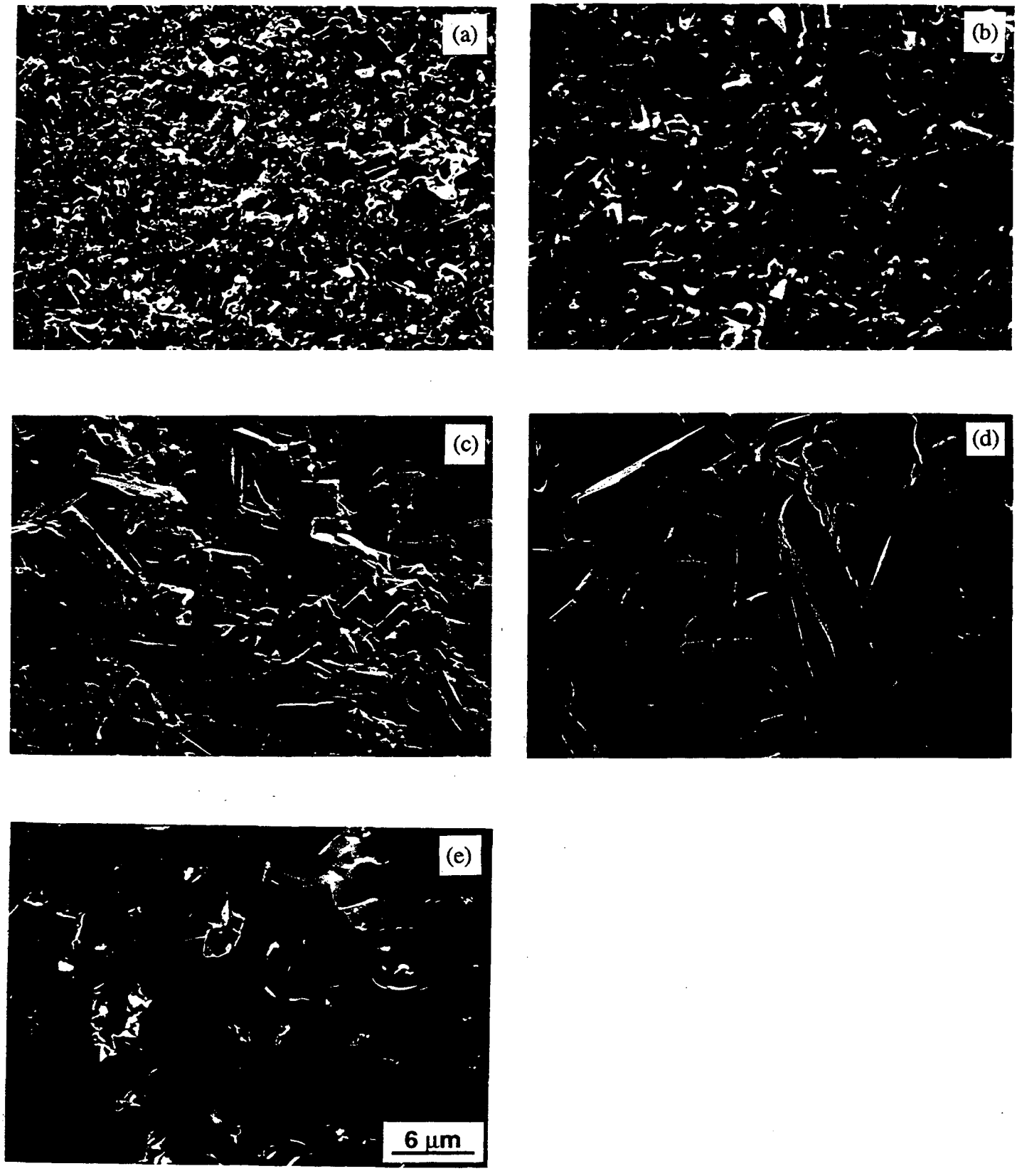

Fig.12 SEM fractographs of silicon carbides hot pressed at various temperatures: (a) 1700°C/1hr; (b) 1780°C/1hr; (c) 1900°C/1hr; (d) 1950°C/1hr; and (e) Hexoloy SiC.

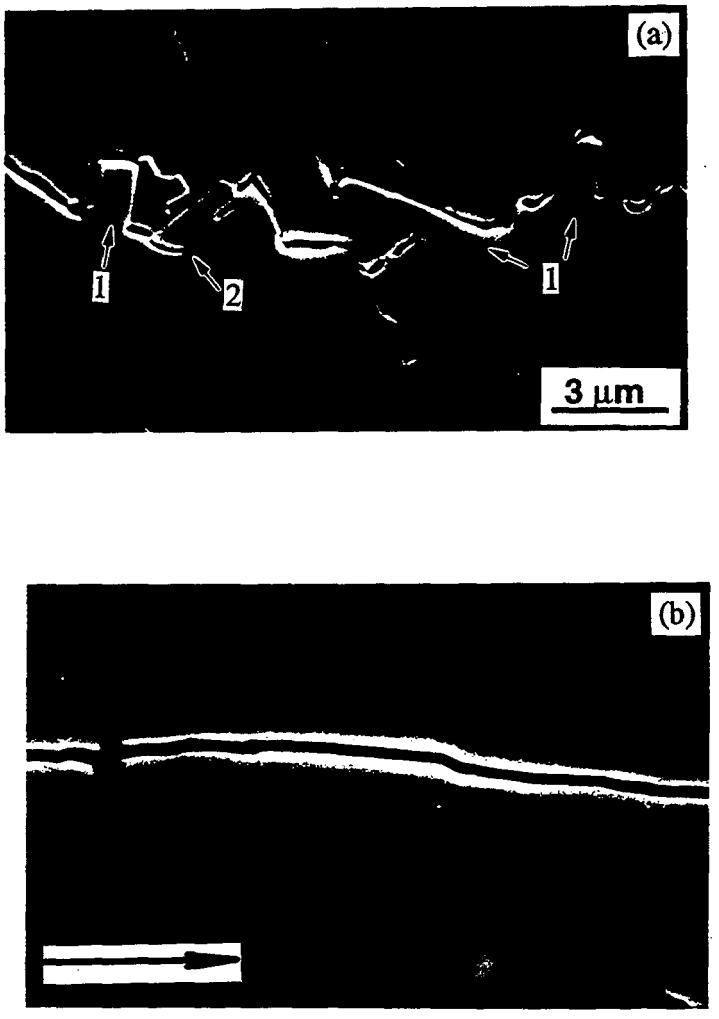

Fig.13 SEM images of crack paths from Vickers indentation in (a) an *in situ* toughened SiC, and (b) Hexoloy SiC. Note the bridged (as shown by arrow 1) and deflected (arrow 2) path in (a), versus the straight and transgranular path in (b). The horizontal arrow shows direction of crack growth.

LAWRENCE BERKELEY LABORATORY
UNIVERSITY OF CALIFORNIA
TECHNICAL INFORMATION DEPARTMENT
BERKELEY, CALIFORNIA 94720